Journal of Physics: Conference Series **80** (2007) 012040 doi:10.1088/1742-6596/80/1/012040

Excited-state imaging of cold atoms

David V Sheludko,[1] Simon C Bell,[1] Edgar J D Vredenbregt,[2] and Robert E Scholten[1]

[1]School of Physics, The University of Melbourne, Victoria 3010, Australia
[2]Physics Department, Eindhoven University of Technology, 5600MB Eindhoven, The Netherlands

E-mail: r.scholten@physics.unimelb.edu.au

Abstract. We have investigated state-selective diffraction contrast imaging (DCI) of cold ^{85}Rb atoms in the first excited ($5^2P_{3/2}$) state. Excited-state DCI requires knowledge of the complex refractive index of the atom cloud, which was calculated numerically using a semi-classical model. The Autler-Townes splitting predicted by the model was verified experimentally, showing excellent agreement.

780 nm lasers were used to cool and excite atoms within a magneto-optical trap, and the atoms were then illuminated by a 776 nm imaging laser. Several excited-state imaging techniques, including blue cascade fluorescence, on-resonance absorption, and DCI have been demonstrated. Initial results show that improved signal-to-noise ratio (SNR) will be required to accurately determine the excited state fraction. We have demonstrated magnetic field gradient compression of the cold atom cloud, and expect that further progress on compression and additional cooling will achieve sufficient diffraction contrast for quantitative state-selective imaging.

1. Introduction

A minimally destructive imaging technique has been developed to determine the fraction and distribution of excited-state ^{85}Rb atoms in a magneto-optical trap (MOT). The work has been motivated by a general interest in probing atomic coherence states and related phenomena such as electromagnetically induced transparency (EIT) [1], coherent frequency upconversion [2], and "slow light" [3]. These phenomena have typically been studied using techniques without spatial resolution, and imaging offers the potential for obtaining much greater information. Combining diffraction-based phase imaging with control of the internal state of the imaged atoms using a probe laser, we can explore techniques for enhancing the imaging (e.g. by modifying the refractive index), or for directly measuring the control process itself.

More specifically, we are interested in measuring the distribution of excited-state atoms in a cold atom cloud, for subsequent application to creating ultra-cold plasma (UCP) with defined spatial distribution [4]. UCP is created by photo-ionisation of an ultra-cold atom cloud (see fig. 1), and the thermal energy of the electrons can be weaker than the electron-ion Coulomb binding. Such strongly-coupled plasmas provide an interesting analogue for astrophysical systems including stellar clusters [5].

The electron cloud can be accelerated and used to produce x-rays via inverse-Compton scattering of a high-intensity laser beam [6, 7]. Existing thermal electron sources (e.g. the photon gun, in which a high intensity 5 ps laser pulse is incident on a copper cathode, producing

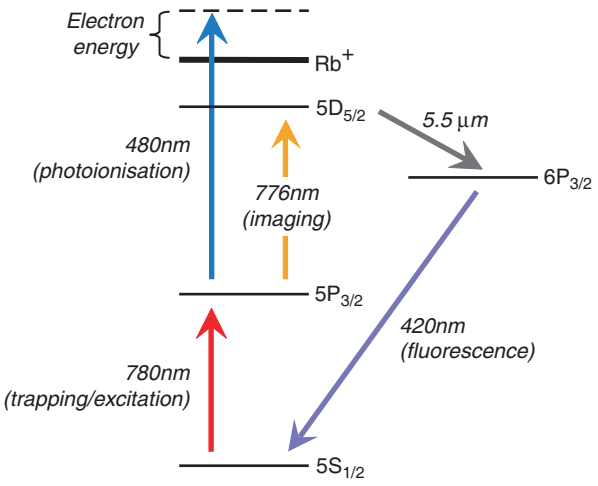

Figure 1. Simplified ^{85}Rb level scheme for production of an ultra-cold plasma and imaging. Atoms are cooled and maintained in the excited 5P state by the 780 nm laser. A 480 nm pulse will photoionise the atoms, producing cold electrons. The excited-state atom distribution will be determined with imaging on the 5P – 5D transition at 776 nm.

thermal electrons [8]) have limited potential in this application due to their broad initial velocity distribution. A cold electron source from an ultra-cold plasma could overcome this limitation, enabling a compact, bright, low-cost alternative to a synchrotron x-ray beamline [9]. However, the x-ray output is critically dependent on the electron density and therefore the initial distribution of electrons, which is determined by the distribution of excited-state cold atoms and the spatial profile of the photoionisation laser. Optimisation of the electron source will require imaging of the excited-state atom distribution, with feedback to the spatial profiles of the cooling and trapping lasers (which also provide excitation), and the photoionisation laser.

Conventional imaging techniques such as on-resonance absorption imaging are simple and effective. They are also highly destructive to the atom cloud and extremely sensitive to experimental parameters such as defocus, detuning of the imaging laser, and optical alignment. Phase imaging techniques, including Zernike phase-contrast, show some promise but are experimentally demanding and quantitative only for a restricted range of phase shifts. Diffraction contrast imaging (DCI) [10] is quantitative, minimally destructive, and less sensitive to experimental parameters than either conventional absorption imaging or classical phase imaging.

Excited-state imaging is experimentally challenging regardless of the imaging method. The expected excitation fraction of the 5P state is 40%. The narrow linewidth of the 776 nm excited-excited transition results in low (5%) absorption of the 776 nm imaging beam. In combination, the signal-to-noise ratio for simple absorption imaging is expected to be 50 times lower than for 780 nm. Fortunately, for the specific case of ultra-cold plasma formation to produce a bright electron source, high atomic density and small cloud size are inherently desirable, both features which will enhance the DCI contrast.

2. Theory

Figure 2 shows the arrangement for diffraction contrast imaging. An off-resonance probe laser beam is incident on a cloud of cold atoms, experiences a spatially dependent absorption and phase shift, and then propagates to a spatially resolving detector such as a CCD camera which records the object diffraction pattern. Algebraic linear inversion of the Fresnel diffraction relation in Fourier space returns a quantitative measurement of the column density of the sample. The

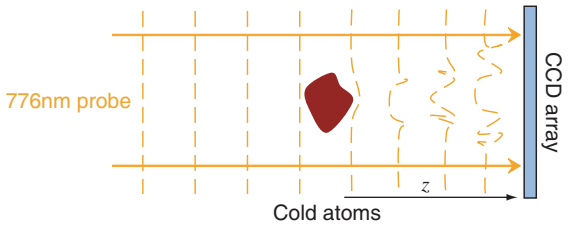

Figure 2. Diffraction contrast imaging records the diffraction pattern of an off-resonant plane wave incident on a cold atom sample.

relation between the Fourier transform of the normalised contrast of the diffraction pattern, $\mathcal{F}\left[(I - I_0)/I_0\right]$, and the Fourier transform of the column density at the object, $\mathcal{F}\left[\rho(\mathbf{x})\right]$, is given by [10]:

$$\mathcal{F}\left[\frac{I - I_0}{I_0}\right] = 2k\left(\delta \sin(\pi\lambda z u^2) - \beta\cos(\pi\lambda z u^2)\right)\mathcal{F}\left[\rho(\mathbf{x})\right] \tag{1}$$

where $k = 2\pi/\lambda$, λ is the wavelength of the probe laser, z is the propagation distance and u is the spatial frequency conjugate to $\mathbf{x}$. δ and β are the phase and absorption coefficients, where $\phi = k\delta\rho$ and $\mu = k\beta\rho$ are the phase shift and absorption of the atomic cloud.

Quantitative retrieval of the column density requires knowledge of the absorption/phase ratio, β/δ, for all (x, y). Previous work [10] has assumed a two-level atom approximation to derive an analytic absorption/phase ratio depending only on the probe detuning. For excited-state imaging, a two-level approximation is not generally appropriate due to the perturbing effect of the excitation laser field. Atoms in the 5P state decay to the ground state via spontaneous emission with a lifetime of approximately 26 ns, much shorter than typical imaging exposure durations (10–50 μs). To maintain atoms in the 5P excited state, the 780 nm cooling (and excitation) beams must remain on, perturbing the atomic eigenstates.

The refractive index of a medium is defined as $n = \sqrt{\epsilon}$, where $\epsilon = 1 + \chi_e$ is the electric permittivity and χ_e the electric susceptibility. For small χ_e, $n \approx 1 + \chi_e/2$ [11]. Treating the atom-field interaction semi-classically, the polarisation $\mathbf{P}$ of a monatomic gas is related to the field $\mathbf{E}$ by $\mathbf{P} = \chi_e\mathbf{E}$. The polarisation of the atomic gas can be determined using a density matrix formalism, where $\mathbf{P}$ is given by the off-diagonal elements of the density matrix for the system, ρ [12]. The density matrix elements were calculated using optical Bloch equations [13] for three-level atoms (5S, 5P, 5D; see fig. 1) with two coupling laser fields. The system is described by six coupled differential equations, which were solved by numerical integration for steady-state conditions. The absorption and phase components of the 776 nm susceptibility are shown in figure 3, for a 780 nm detuning of -3Γ. Autler-Townes energy level splitting [14] is evident in the predicted spectrum of the 776 nm laser, caused by the strong perturbing influence of the applied 780 nm field. The splitting was observed to increase as expected with increased 780 nm detuning or increased 780 nm power.

Atoms that are in the $5D_{5/2}$ state can decay not only to the $5P_{3/2}$ state, but also to the $6P_{3/2}$ state, emitting a 5 μm photon. From this state, they decay back to the ground state, releasing a 420 nm blue photon (fig. 1). The absorption of the 776 nm beam is proportional to the 420 nm fluorescence, which can be readily measured and compared to the theoretical prediction of Autler-Townes splitting.

3. Experiment

The experimental arrangement consists of a vapour cell magneto-optical trap (MOT) in a $\sigma^{\pm}$ (circularly polarised) arrangement [15, 16]. Cooling and trapping was performed on the $5S_{1/2}\,F = 3 \rightarrow 5P_{3/2}\,F' = 4$ hyperfine transition of ^{85}Rb, with external-cavity diode lasers

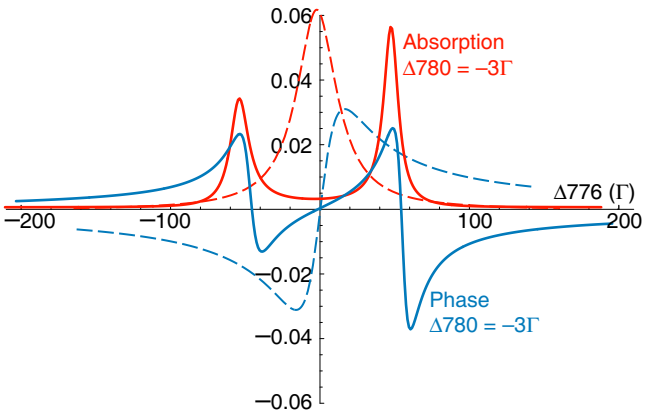

Figure 3. Phase and absorption on the 776 nm transition for a three-level model of Rb. The two-level results (dashed) are clearly not valid for excited-state imaging.

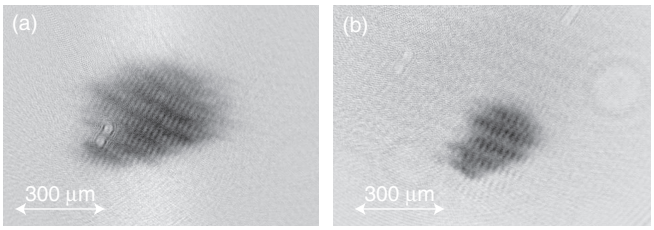

Figure 4. 780 nm absorption images showing compression due to increase in magnetic field gradient. (a) no compression, field gradient 10 G/cm; (b) after 100 ms compression to 50 G/cm. Cloud full width at half maximum from Gaussian fit, 735 ± 20 μm and 322 ± 12 μm respectively. Both images: 10 ms exposure, 20 μs pulse duration, 1.5 mW probe beam power, getter current 4.2 A.

(ECDLs) frequency stabilised using saturated absorption spectroscopy [17, 18]. A master oscillator power amplifier (MOPA) provided a total cooling beam power of 150 mW at the MOT, after fibre coupling. The cooling beam diameter at the MOT was approximately 20 mm.

Anti-Helmholtz coils provided a field gradient of 10 G/A cm with a maximum of 6 A. An additional 780 nm repump laser, locked to the $F = 2 \rightarrow F' = 3$ hyperfine transition, was copropagated along one axis of the cooling beams. Rubidium atoms were provided by a getter source.

Inital 776 nm imaging results exhibited poor SNR. To increase the atomic density, a compressed MOT (CMOT) technique was employed [19]. Initially, the coils (and hence the trap) were off, to record a background image. The getter was then driven at high current, and the coils set at 1 A (10 G/cm) for 30 s to load the trap. The coil current was ramped to a variable maximum (up to 60 G/cm) over times ranging from 5 ms to several seconds. An image was acquired, and the getter then returned to a low current (2.5 A) and the coils turned off.

A comparison of images taken before and after compression is shown in figure 4. Spatial compression of the MOT is clearly apparent, with a peak magnetic field gradient of 50 G/cm compressing the MOT to approximately half the 10 G/cm diameter. The compression was negligible for field gradients below 30 G/cm and also showed only marginal improvement for higher field gradients of 60 G/cm, consistent with findings reported elsewhere [19]. In addition, the cooling beams may be further detuned to provide additional cooling and higher density. This technique has the potential to increase the density by an order of magnitude when completed,

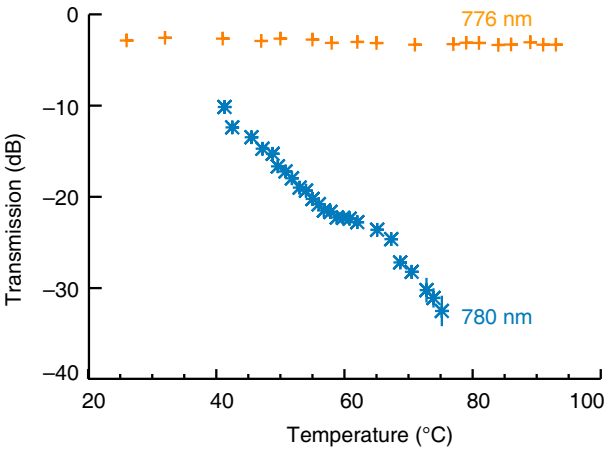

Figure 5. Attenuation of 780 nm and 776 nm light by a heated 10 cm vapour cell narrow-bandwidth atomic filter.

which we expect to be sufficent for quantitative DCI.

Because the cooling beams are left on during 776 nm imaging, 780 nm fluorescence creates a strong background, substantially reducing the image contrast for 776 nm in-focus absorption imaging, and completely saturating blue fluorescence imaging. To separate the imaging probe beam (at 776 nm) from the fluorescence (at 780 nm, i.e. only 4 nm apart) a very narrow bandpass filter was required.

A novel filter was created from a heated rubidium vapour cell. Absorption of the 780 nm fluorescence was much stronger than on the 776 nm probe beam, and a 10 cm vapour cell at 85°C was able to reduce the 780 nm fluorescence to immeasurable intensity in a one second exposure. A plot of the attenuation of 776 nm and 780 nm light versus temperature is shown in figure 5. In addition, a hot/cold filter (Thorlabs FM03, $< 10\%$ transmission below 630 nm) was used during 776 nm absorption imaging to remove any blue fluorescence. Both filters were removed for 780 nm imaging.

To verify the theoretically predicted Autler-Townes splitting, the blue MOT fluorescence at 420 nm was recorded as the 776 nm laser was scanned through a frequency range of approximately 180 MHz. The measurement was performed for several 780 nm cooling beam detunings, from -25 MHz to -10 MHz. The resulting spectra and the theoretical predictions are shown in figure 6.

The spectra obtained are in good agreement with the theory. The small shoulder on the right edge of the large peak in the $\Delta_{780} = +20$ MHz spectrum is believed to be due to hyperfine splitting of the 5D state, which was clearly visible on the locking absorption signal. The observed separation of approximately 10 MHz is consistent with published values of the 5D hyperfince splitting [20]. The excellent agreement for the Autler-Townes splitting provides confidence that our Bloch equation model can reliably calculate the detuning dependence of the refractive index for the 776 nm transition.

Blue fluorescence images were taken using the heated rubidium vapour cell to remove 780 nm fluorescence. The hot/cold filter was removed for these images, and the trapping beams remained on at all times. A control image with the 776 nm beam blocked was taken immediately after every blue fluorescence frame, to ensure that any cooling of the vapour cell had not allowed 780 nm light to contaminate the image. An example image, its control image and the corresponding line profile is shown in figure 7. Due to the long exposure time required, fluorescence images showed considerable blurring, lowering the spatial resolution and preventing their use for quantitative imaging.

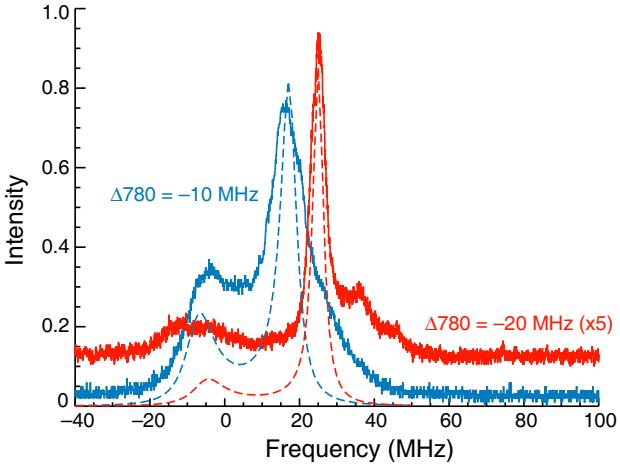

Figure 6. Theoretical (dashed) and experimental (solid) 420 nm fluorescence in the MOT for 780 nm cooling beam detunings of -10.0 ± 0.5 and -20 ± 3 MHz.

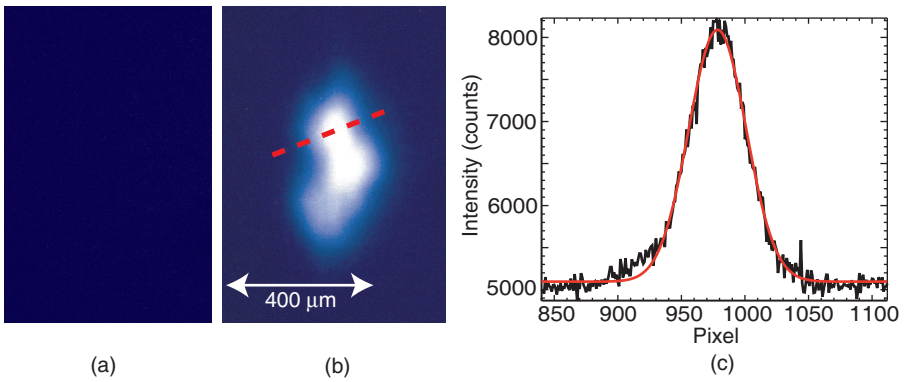

Figure 7. Blue fluorescence image of the MOT for 780 nm excitation and 776 nm probe. (a) Control image with 776 nm beam off. (b) Blue fluorescence image (false colour). 1 second exposure with 4.12 A getter current, 2.1 A coil current (21 G/cm), 85°C vapour cell filter temperature. (c) Line profile along the dotted red line in (b) with Gaussian fit.

On-resonant in-focus 776 nm absorption images were also obtained (fig. 8). While the contrast was still too poor to provide a definitive measurement of the fraction or distribution of excited atoms, the presence of absorption indicates the viability of the technique and can be used to provide an estimate of the column density required for a quantitative measurement.

Considerable noise and fringing is present in the image, caused mainly by the many uncoated optical surfaces of the vapour cell and hot/cold filter used in the beam line. As expected, the best images resulted from long exposures and pulse times, with probe power approximately 150 μW. From the line profile in figure 8, the SNR is approximately 0.8. A 780 nm absorption image with similar image parameters has SNR an order of magnitude greater, indicating an order of magnitude increase in column density is required to obtain a similar imaging result at 776 nm. The peak column density of the atom cloud is 4.7×10^{13} m^{-2}. The increased density is required for planned experiments on ultra-cold plasma and atomic coherence and can be achieved using additional cooling as described with the CMOT technique earlier.

As anticipated from the results of the 776 nm absorption images, a higher density is also needed to provide the necessary contrast for quantitative excited-state DCI. An excited-state

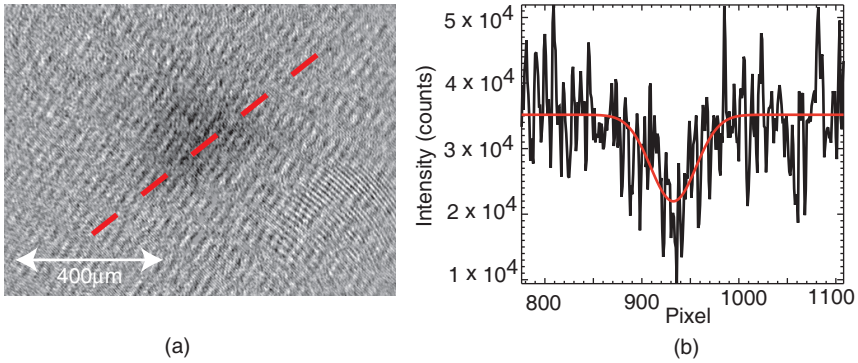

Figure 8. (a) In-focus absorption image of atoms in the 5P state using 776 nm probe beam. Experimental parameters: 4.2 A getter current, 2.2 A coil current (22 G/cm), 150 μW probe beam power, 300 μs pulse duration, 1 ms exposure, 85°C cell temperature. (b) Line profile and Gaussian best-fit through the dashed red line in (a).

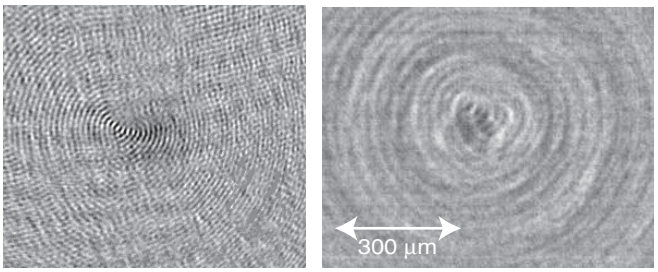

Figure 9. 776 nm DCI diffraction pattern (left) and column density retrieval (right). Experimental parameters: 4.1 A getter current, 4.1 A coil current, 150 μW probe beam power, 80 μs pulse duration, 100 ms exposure, +2Γ detuning from absorption peak, 50 mm effective defocus. Diffraction is not discernible in the raw data and consequently the atomic cloud is not apparent in the recoverd image.

diffraction pattern and its column density reconstruction is shown in figure 9. The diffraction is too weak to support DCI. Despite the lack of a quantitative result at this early stage, the techniques for achieving the required column density are proven and are planned for the near future.

4. Conclusion

Diffraction-contrast imaging offers a simple yet powerful method for imaging cold atom samples. Quantitative imaging requires knowledge of the ratio of the real to imaginary components of the refractive index of the sample, which we have calculated for the three-level two-laser system using a semi-classical approach. The model also predicted Autler-Townes splitting of the rubidium 5P excited state, which was found to be in good agreement with experimental measurements.

We have investigated the feasibility of imaging excited state cold atoms in a MOT, using a variety of techniques. Blue fluorescence imaging provided a good signal-to-noise ratio, but poor resolution and an imprecise measurement of the excited state fraction. On-resonance absorption imaging provides low spatial resolution information which will improve with higher atomic density, which may also enable effective diffraction contrast imaging.

We have demonstrated that with careful optimisation of atomic column density, DCI has the potential to provide quantitative information about the fraction and distribution of excited

state atoms. In future work, we will implement additional cooling and compression of the atomic sample, to reduce the cloud size and increase the atomic density. We will investigate imaging in conjunction with atomic coherence effects, such as electromagnetically induced transparency and "slow light". More directly, we intend to improve the technique for use in optimisation of an ultra-cold plasma. The many possible applications for this technique make it a valuable tool for atom optics research.

This research was supported under the Discovery funding scheme of the Australian Research Council (project DP0557505).

[1] Hopkins S A, Usadi E, Chen H X and Durrant A V 1997 *Opt. Comm.* **138** 185
[2] Meijer T, White J D, Smeets B, Jeppesen M and Scholten R E 2006 *Opt. Lett* **31** 1002
[3] Hau L V, Harris S E, Dutton Z and Behroozi C H 1999 *Nature* **397** 594.
[4] Killian T C, Kulin S, Bergeson S D, Orozco L A, Orzel C and Rolston S L 1999 *Phys. Rev. Lett.* **83** 4776
[5] Comparat D, Vogt T, Zahzam N, Mudrich M and Pillet P 2004 *Mon. Not. R. Astron. Soc.* **361** 1227
[6] Carroll F 2003 *J. Cell. Biochem.* **90** 502
[7] Milburn R H 1963 *Phys. Rev. Lett.* **10** 75
[8] Carroll F E, Mendenhall M H, Traeger R H, Brau C and Waters J W 2003 *Am. J. Roentgen.* **181** 1197
[9] Claessens B J, van der Geer S B, Taban G, Vredenbregt E J D and Luiten O J 2005 *Phys. Rev. Lett.* **95** 4801
[10] Turner L D, Domen K F E M and Scholten R E 2005 *Phys. Rev. A* **72** 1403
[11] Loudon R 2000 *The Quantum Theory of Light* 3rd edn (Oxford: Oxford University Press)
[12] Scully M O and Zubairy M S 1997 *Quantum Optics* (Cambridge: Cambridge University Press)
[13] Maguire L P, van Bijnen R M W, Mese E and Scholten R E 2006 *J. Phys. B: At. Mol. Opt. Phys.* **39** 2709
[14] Autler S H and Towne C H 1955 *Phys. Rev.* **100** 703
[15] Metcalf H J and van der Straten P 1999 *Laser Cooling and Trapping* (Berlin: Springer-Verlag) .
[16] Wieman C, Flowers G and Gilbert S 1995 *Am. J. Phys.* **63** 317
[17] Hawthorn C J, Weber K P and Scholten R E 2001 *Rev. Sci. Inst.* **72** 4477
[18] Turner L D, Weber K P, Hawthorn C J and Scholten R E 2002 *Opt. Commun.* **201** 391
[19] Petrich W, Anderson M H, Ensher J R and Cornell E A 1994 *JOSA B* **11** 1332
[20] Nez F, Biraben F, Felder R and Millerioux Y 1993 *Opt. Commun.* **102** 432